MOLECULAR AND CELLULAR BIOLOGY, Aug. 1996, p. 4172–4181 Vol. 16, No. 8
0270-7306/96/$04.00+0


# Interaction of the Interferon-Induced PKR Protein Kinase with Inhibitory Proteins P58$^{IPK}$ and Vaccinia Virus K3L Is Mediated by Unique Domains: Implications for Kinase Regulation

MICHAEL GALE, JR., SENG-LAI TAN, MARLENE WAMBACH, AND MICHAEL G. KATZE*

*Department of Microbiology, School of Medicine, and Regional Primate Research Center, University of Washington, Seattle, Washington*

Received 5 March 1996/Returned for modification 26 April 1996/Accepted 9 May 1996

**Expression of the double-stranded RNA-activated protein kinase (PKR) is induced by interferons, with PKR activity playing a pivotal role in establishing the interferon-induced antiviral and antiproliferative states. PKR is directly regulated by physical association with the specific inhibitor, P58$^{IPK}$, a cellular protein of the tetratricopeptide repeat (TPR) family, and K3L, the product of the corresponding vaccinia virus gene. P58$^{IPK}$ and K3L repress PKR activation and activity. To investigate the mechanism of P58$^{IPK}$- and K3L-mediated PKR inhibition, we have used a combination of in vitro and in vivo binding assays to identify the interactive regions of these proteins. The P58$^{IPK}$-interacting site of PKR was mapped to a 52-amino-acid aa segment (aa 244 to 296) spanning the ATP-binding region of the protein kinase catalytic domain. The interaction with PKR did not require the C-terminal DNA-J homology region of P58$^{IPK}$ but was dependent on the presence of the eukaryotic initiation factor 2-α homology region, mapping to the 34 aa within the sixth P58$^{IPK}$ TPR motif. Consistent with other TPR proteins, P58$^{IPK}$ formed multimers in vivo: the N-terminal 166 aa were both necessary and sufficient for complex formation. A parallel in vivo analysis to map the K3L-binding region of PKR revealed that like P58$^{IPK}$, K3L interacted exclusively with the PKR protein kinase catalytic domain. In contrast, however, the K3L-binding region of PKR was localized to within aa 367 to 551, demonstrating that each inhibitor bound PKR in unique, nonoverlapping domains. These data, taken together, suggest that P58$^{IPK}$ and K3L may mediate PKR inhibition by distinct mechanisms. Finally, we will propose a model of PKR inhibition in which P58$^{IPK}$ or a P58$^{IPK}$ complex binds PKR and interferes with nucleotide binding and autoregulation, while formation of a PKR-K3L complex interferes with active-site function and/or substrate association.**

Eukaryotic protein kinases are regulated by a variety of mechanisms, including but not limited to transcriptional activation (55), association with activating subunits (19), and phosphorylation (64). The relationship between the mammalian cyclin-dependent kinases (CDKs) and their cognate cellular inhibitors of the p21/p27 (29, 65) and p16/p18 (27) families defines a less common mechanism of protein kinase regulation. This mechanism involves inhibition of catalytic activity by the direct physical association with a specific inhibitory protein (1). Direct physical interaction between CDK inhibitors and CDK or the CDK-cyclin complex occurs during the cell cycle and in response to growth-regulating signals, with complex formation necessary for CDK inhibition (29, 56). Similarly, activity of the double-stranded RNA (dsRNA)-activated serine/threonine protein kinase, PKR, is regulated in part by association with specific inhibitory proteins, including a cellular inhibitor, previously referred to as P58 (51, 66), which we now designate P58$^{IPK}$ (for 58-kDa inhibitor of protein kinase). PKR is unique among protein kinases in that, in addition to being regulated by a cellular inhibitor, it is the target for regulation by virally encoded inhibitory molecules (37).

Constitutively expressed at low levels, PKR plays a pivotal role in the regulation of mRNA translation (30, 36, 60, 68). As one of over 30 interferon-inducible genes, PKR is a key participant in the establishment of the interferon-mediated cellular antiviral and antiproliferative responses (37, 38, 70). By binding dsRNA, PKR undergoes a conformational change and becomes autophosphorylated (22), an event that may be mediated by PKR homodimerization (48, 75). Once activated, the kinase phosphorylates serine 51 on the alpha subunit of eukaryotic initiation factor 2 (eIF2-α) which leads to a limitation in functional eIF2 and a resultant block in protein synthesis initiation (60). The role of PKR is best understood in viral systems in which virus-specific RNAs, with intrinsic secondary structure, have the potential to activate the kinase (36). Eukaryotic viruses must therefore suppress PKR activity or otherwise encounter declines in protein synthesis rates resulting in inhibition of viral replication (38). Thus, many viruses have developed mechanisms to repress PKR activity (reviewed in reference 38). Examples include the adenovirus-encoded VAI RNA, which forms an inhibitory complex with PKR by functioning as a competitive inhibitor of dsRNA binding (39). Both reovirus and vaccinia virus encode virus-specific dsRNA-binding proteins which function to sequester dsRNA activators of PKR (14, 34). In addition, the 88-amino-acid (aa) *K3L* gene product of vaccinia virus, K3L, and the *tat* gene product of human immunodeficiency virus type 1 form a physical complex with PKR resulting in inhibition of kinase activity during viral infection (13, 59, 69). Mutant vaccinia virus lacking K3L possesses an interferon-sensitive phenotype due, in part, to a failure to inactivate PKR, thereby resulting in a dramatic reduction in virus production (7).

Influenza virus encodes a novel mechanism to repress PKR activity: virus infection results in the activation of the cellular

* Corresponding author. Mailing address: University of Washington, Dept. of Microbiology, Box 357242, Seattle, WA 98195. Phone: (206) 543-8837. Fax: (206) 685-0305. Electronic mail address: honey@u.washington.edu.

58-kDa PKR inhibitor known as P58, herein designated as P58$^{IPK}$ (40, 51–53). P58$^{IPK}$ is a member of the tetratricopeptide repeat (TPR) family of proteins (25, 51), possessing nine tandemly arranged TPR motifs, which are known to mediate both homotypic and heterotypic protein-protein interactions (47). In addition, P58$^{IPK}$ possesses a C-terminal DNA-J motif, which likewise has been implicated in mediating protein-protein interactions (71). P58$^{IPK}$ is constitutively expressed in mammalian cells (44, 51) but resides in an inactive complex with a specific inhibitor termed I-P58$^{IPK}$ (53). Like K3L, activated P58$^{IPK}$ forms a physical complex with PKR, resulting in inhibition of both PKR phosphorylation and activity (66). Both P58$^{IPK}$ and K3L have limited homology to eIF2-α, suggesting that they may utilize a common mechanism of PKR inhibition. While the mechanism of kinase inhibition by each of these PKR inhibitors is currently unknown, it has been proposed that K3L inhibits PKR by functioning as a protein kinase pseudosubstrate, blocking the PKR-eIF2-α substrate interaction (7, 8, 13).

To begin to understand the mechanisms of cellular and virus-mediated regulation of PKR, we have undertaken a structural analysis of the PKR-P58$^{IPK}$ and PKR-K3L interactions, as well as an assessment of P58$^{IPK}$ homotypic interactions. We can now demonstrate that P58$^{IPK}$ forms a stable complex with PKR in vivo. In addition, we found that, like other TPR proteins, P58$^{IPK}$ is capable of self-association, forming stable homotypic complexes in vivo. The association with PKR was mapped to within the sixth TPR repeat motif of P58$^{IPK}$. While the N terminus of P58$^{IPK}$ was not required for interaction with PKR, it was required for self association. Thus, the P58$^{IPK}$ domains which mediate homotypic and the PKR heterotypic interaction are independent. Finally, we found that P58$^{IPK}$ bound to a discrete region of the PKR protein kinase catalytic domain, which was distinct from the region which interacted with the vaccinia virus PKR-inhibitory protein, K3L.

## MATERIALS AND METHODS

**Plasmids and constructs.** Construction of the PKR mutants PKR Δ362-367 in pCDNA1neo (Invitrogen) and of PKR K296R, PKR 1-296, and PKR 244-551 in pET11a (Novagen) and pCDNA1neo was previously described (4, 17, 41, 43). For construction of GAL4 transcriptional activation domain (AD) and GAL4 DNA-binding domain (BD) fusions, the *Nde*I linker sequence, ccatatgg, was ligated into the *Sma*I site of pGAD424 (AD) and pGBT9 (BD; Clontech) to generate pGAD425 and pGBT10, respectively. Plasmid inserts encoding PKR K296R, PKR 1-296, and PKR 244-551 were released from pET11a by cleaving with restriction enzymes *Nde*I and *Bam*HI. The resultant inserts were gel purified and cloned into *Nde*I-*Bam*HI-digested pGAD425 to yield pAD-PKR K296R, pAD-PKR 1-296 and pAD-PKR 244-551, respectively. A *Bam*HI fragment encoding the N-terminal 242 aa of PKR was introduced into the *Bam*HI site of pGAD424 to produce pAD-PKR 1-242. pAD-PKR 367-551 was constructed by cleaving pAD-PKR 244-551 with restriction enzyme *Eco*RI and religating the cleaved plasmid to produce an in-frame fusion deleting aa 244 to 366. Construction of pAD-PKR 244-366 was facilitated by cloning the *Eco*RI fragment from pAD-PKR 244-551 into *Eco*RI-digested pGAD424. To construct pAD-PKR 244-296, nucleotides (nt) 729 to 887 of the PKR coding region (61) were amplified from pAD-PKR 242-551 by PCR using the restriction site-linked oligonucleotide primers pair 5′ gagatcgaattcccc<u>catatg</u>gcacccaga 3′ (sense primer; *Nde*I site underlined) and 5′ acgcg<u>gctgcag</u>ctatttaataacgtaagtctttccgtc 3′ (antisense primer; *Pst*I site underlined). Following amplification, the PCR product was cleaved with *Nde*I and *Pst*I and subsequently cloned into *Nde*I-*Pst*I-digested pGAD425. pGST-P58$^{IPK}$ encodes bovine wild-type P58$^{IPK}$ (P58$^{IPK}$) fused to glutathione *S*-transferase (GST) in pGEX2T (72). Production of pBD-P58$^{IPK}$ was as follows. The coding region of human P58$^{IPK}$wt was amplified by PCR using the sense oligonucleotide primer 5′ at<u>gaattc</u>atggtggcccccggctccg 3′ (*Eco*RI linker underlined), corresponding to P58$^{IPK}$ nt 1 to 19, and the antisense primer 5′ cgcc<u>ggatccgg</u>tttaattgaagtggaattt 3′ (*Bam*HI linker underlined), corresponding to P58$^{IPK}$ nt 1498 to 1518. Following amplification, the PCR product was cleaved with restriction enzymes *Eco*RI and *Bam*HI and ligated into *Eco*RI-*Bam*HI-cleaved pGAD424 and pGBT9 to produce pAD- and pBD-P58$^{IPK}$. To eliminate the possibility of PCR-generated mutations, the internal *Bst*XI-*Bam*HI fragment was released from pBD-P58$^{IPK}$ and replaced with the *Bst*XI-*Bam*HI fragment from pCDNA1neo-P58$^{IPK}$ (2) to generate pBD-P58$^{IPK}$wt. The construction of the P58$^{IPK}$ mutants 8-1 (aa 1 to 166), 8-2 (aa 1 to 277), and 9-1 (aa 168 to 504) has been described elsewhere (51). P58$^{IPK}$ mutant P58$^{IPK}$/ΔTPR6 (aa 222 to 255 deleted) in pCDNA1neo was a gift from N. Tang and is described in a separate report (73). Plasmid inserts encoding P58$^{IPK}$ mutants 8-1, 8-2, and P58$^{IPK}$/ΔTPR6 were recovered by carrying out internal *Bst*XI-*Bam*HI digests. The resulting DNA fragments were gel purified and cloned into *Bst*XI-*Bam*HI-digested pAD- and pBD-P58$^{IPK}$ to give the respective AD and BD plasmids of 8-1, 8-2, and P58$^{IPK}$/ΔTPR6. DNA encoding P58$^{IPK}$ mutant 9-1 was recovered by *Nde*I-*Bam*HI digestion and cloned into *Nde*I-*Bam*HI-digested pGAD425 and pGBT10 to give pAD- and pBD-9-1, respectively. Plasmid pBD-K3L encodes the entire open reading frame of the vaccinia virus (Wisconsin strain) *K3L* gene product K3L, fused to the GAL4 BD and was a generous gift from R. Jagus.

**In vitro transcription and translation.** Transcripts encoding full-length and mutant PKR and P58$^{IPK}$ were generated essentially as described previously (41), using the T7 promoter of pCDNA1neo or pET15b (Novagen). Linear transcripts encoding full-length PKR (K296R), PKR aa 1 to 296 or 244 to 551, or the PKR Δ362-367 mutant (aa 362 to 367 deleted) were generated from the corresponding *Eco*RV-digested pCDNA1neo construct. Transcripts encoding PKR aa 1 to 242 and 1 to 384 were generated by linearizing pCDNA1neo-PKR K296R at the PKR-internal restrictions sites *Ban*I and *Mae*I, respectively. Transcripts encoding full-length P58$^{IPK}$wt and P58$^{IPK}$ deletion mutant 8-1 were generated from the respective *Xba*I-digested pCDNA1neo constructs. Transcripts from P58 mutant 9-1 were derived from *Bam*HI-cleaved pET15b. Transcript integrity was monitored by agarose gel electrophoresis.

Two micrograms of each in vitro transcription product was used to program a rabbit reticulocyte lysate in vitro translation system (Promega) in the presence of [$^{35}$S]methionine as described previously (41). To verify that the translation products were of the expected sizes, an aliquot of each was analyzed by sodium dodecyl (SDS)-sulfate polyacrylamide gel electrophoresis (PAGE) and fluorography. Translation product abundance was quantitated by scintillation counting of the trichloroacetic acid-precipitable material from each translation reaction.

**In vitro binding assays.** Protein complex formation in vitro was determined by a GST pull-down assay. Overnight cultures of *Escherichia coli* harboring pGEX2T (GST) or pGEX2T-P58$^{IPK}$ (GST-P58$^{IPK}$) were induced with isopropylthiogalactopyranoside for 3 h, and extracts were prepared essentially as described previously (72) except that the cells were resuspended in binding buffer (phosphate-buffered saline, 20 μg of aprotinin per ml, 10 μg of leupeptin per ml, 1 mM phenylmethylsulfonyl fluoride [pH 7.2]) prior to sonication. For analysis of protein interaction, $2.5 \times 10^5$ cpm of the indicated $^{35}$S-labeled in vitro translation product was added to increasing amounts of GST and GST-P58$^{IPK}$ recombinant *E. coli* extracts in a final volume of 500 μl of binding buffer. After 15 min at 30°C, 50 μl of glutathione-agarose beads (50% solution in binding buffer) was added, and the mixture was incubated for 1 h on a 4°C rotator. Following incubation, the reaction mixtures were pelleted in a 4°C microcentrifuge and washed five times with cold binding buffer in the presence of 0.1% Triton X-100. Following the final wash, the glutathione-agarose beads were resuspended in 2× SDS-PAGE sample buffer and incubated in a 100°C bath for 5 min. After a brief centrifugation, supernatants were subjected to SDS-PAGE on 14% acrylamide gels. In vitro translation products which bound to GST or GST fusion proteins were visualized by autoradiography of the dried gel.

**DNA sequence analysis.** The reading frames of all plasmid constructs were verified by nucleotide sequence analysis using the dideoxy method of either the Sequenase kit (version 2.0; Upstate Biotechnology Inc.) or the Applied Biosystems dye terminator system. The insert of construct pAD-PKR 244-296 was sequenced in its entirety to ensure that no mutations were introduced during the cloning process.

**Yeast strains and the yeast two-hybrid assay.** The yeast two-hybrid system (21) was used to assay for in vivo protein-protein interactions. *Saccharomyces cerevisiae* Hf7c [*MAT***a** *ura3-52 his3-200 lys2-801 ade2-101 trp1-901 leu2-3,112 gal4-542 gal80-538 LYS2*::*GAL1-HIS3 URA3*::(*GAL4* 17-mers)$_3$-*CYC1-lacZ*; Clontech] was transfected with the indicated combination of AD and BD plasmids via the lithium acetate method (6). All colonies which contained expression constructs were tested for respective fusion protein expression by immunoblot analysis prior to the two-hybrid assay (see below). The apparent strength of protein-protein interactions as measured in the yeast two-hybrid system is subjected to reporter gene promoter bias of the interacting partners, with identification of specific interactions clearly dependent upon the choice of reporter gene used (20). To minimize this limitation, we chose to use the dual-reporter system of histidine (His) and β-galactosidase (β-Gal) contained in yeast strain Hf7c. In this strain, physical interaction of AD and BD fusion proteins results in the induction of His and β-Gal reporter gene expression. Transfectants were plated onto synthetic defined (SD) medium lacking tryptophan and leucine but containing histidine (+His medium) and incubated for 3 days at 30°C. The resultant colonies were streaked onto SD lacking tryptophan, leucine, and histidine in the presence of 3-aminotriazole (3-AT) (−His medium) and allowed to grow at 30°C for 2 to 4 days to deplete endogenous histidine stores. Colonies were then replica plated onto +His and −His plates and allowed to incubated for 3 days at 30°C, after which the plates were scored for growth. Using 3-AT, a competitive inhibitor of His biosynthesis (42), we found we could alter the stringency of the selection process for interaction. Thus, all cotransfectants were plated onto −His media containing titrated amounts of 3-AT to use the highest possible stringency for

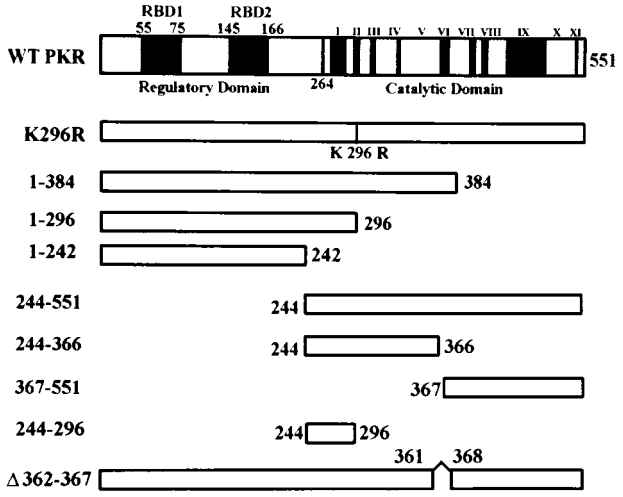


FIG. 1. Structural representation of domain structures of wild-type (wt) PKR (above) and PKR deletion constructs (below). RBD1 and RBD2 denote the positions of the dsRNA-binding motifs 1 and 2, respectively. 264 denotes the amino acid position marking the beginning of the protein kinase catalytic domain in which the positions of the conserved protein kinase homology regions (28) are labeled I to XI. Positions of terminal amino acids are indicated.

each assay (data not shown). Data are reported from the high-stringency (highest 3-AT concentration which supported growth) plates only. Liquid β-Gal assays using the fluorogenic substrate 4-methylumbelliferyl-β-D-galactoside (MUG; Sigma) were carried out on yeast cotransfectants and controls as described previously (12, 24) except that yeast cells were lysed by the glass bead method (see below). Data are reported as the mean increase MUG activity over that of control cotransfectants containing the AD and BD vectors only.

**Immunoblot analysis.** Expression of GAL4 fusion constructs in yeast transfectants was verified by immunoblot analysis using the indicated antibodies and enhanced chemiluminescence (Amersham) as described previously (2, 3). Yeast protein extracts were prepared from 5-ml cultures of each yeast transfectant. Overnight cultures of yeast transfectants in liquid SD medium were transferred to 5 ml of YPD medium at a final optical density at 600 nm of 0.2 and incubated at 30°C until the cultures reached a final optical density at 600 nm of 0.8 (approximately 6 to 8 h). Cells were harvested by centrifugation, resuspended in 1.5 ml of water containing 0.1 mM phenylmethylsulfonyl fluoride, transferred to a microcentrifuge tube, and pelleted in a microcentrifuge. Cell pellets were resuspended in an equal volume of chilled 2× SDS sample buffer and acid-washed glass beads (Sigma) in the presence of 0.1 mM phenylmethylsulfonyl fluoride. Cells were lysed by vortexing three times, each in 30-s bursts, with chilling between each burst. Following lysis, extracts were placed in a 100°C bath for 5 min. Equal volumes of recombinant extracts were separated by SDS-PAGE and blotted to nitrocellulose membranes for immunoblot analysis.

## RESULTS

**PKR and P58$^{IPK}$ form a physical complex in vivo.** Earlier work from the laboratory had demonstrated that P58$^{IPK}$ inhibited PKR activity in vitro, likely through protein-protein interactions (51–53, 66). To determine whether P58$^{IPK}$ and PKR interact in vivo and to precisely map the interactive sites, the following series of experiments were performed. The PKR and P58$^{IPK}$ constructs shown in Fig. 1 and 5, respectively, were expressed as GAL4 AD and BD fusion proteins in yeast cells and tested for in vivo complex formation in the yeast two-hybrid assay (21). Since wild-type PKR is growth suppressive in *S. cerevisiae* (17), the full-length AD-PKR construct was generated from a catalytically inactive mutant, PKR K296R (17, 61). Immunoblot analysis revealed that AD-PKR K296R and BD-P58$^{IPK}$wt constructs were efficiently expressed in transfected yeast clones (Fig. 2A). We used growth on −His medium as our assay for determining interactions in the two-hybrid system. In this assay, growth on −His medium is supported only when the two hybrid proteins interact and in-

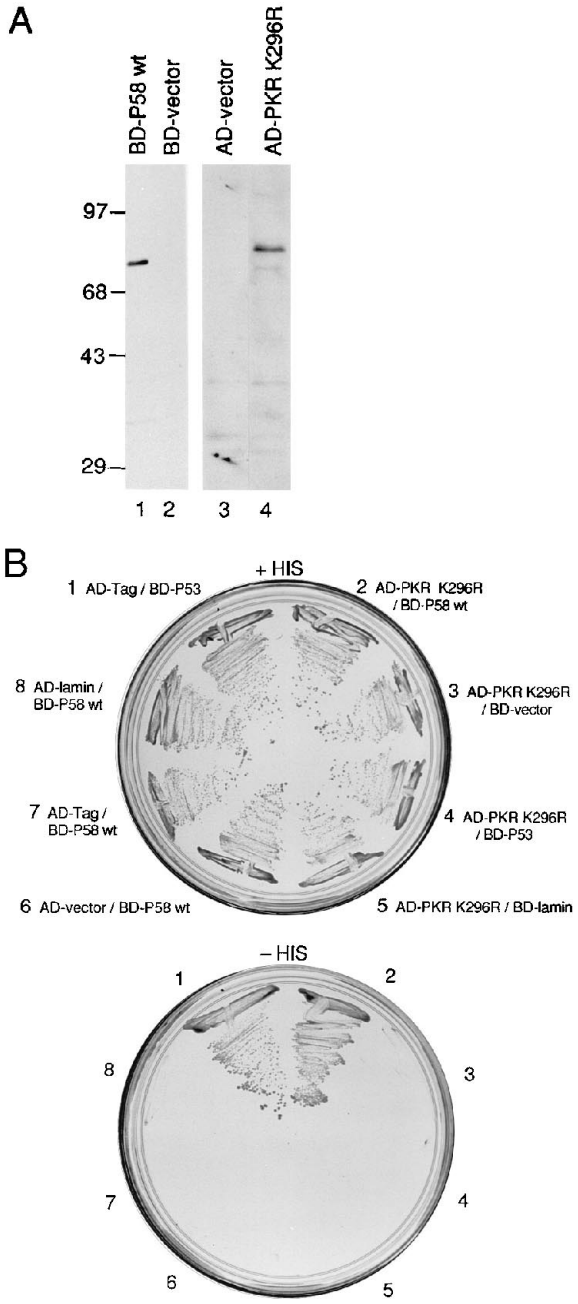


FIG. 2. Full-length PKR and P58$^{IPK}$ physically interact in vivo. (A) Expression of full-length PKR and P58$^{IPK}$ constructs in yeast strains. Shown is immunoblot analysis of extracts prepared from yeast transfectants containing either BD-P58$^{IPK}$wt (lane 1), BD vector (pGBT9 control; lane 2), AD vector (pGAD425 control; lane 3), or AD-PKR K296R (lane 4). The autoradiogram shows blots which were probed with P58$^{IPK}$-specific monoclonal antibody 2F8 (2) (lanes 1 and 2) or a PKR-specific monoclonal antibody (49) (lanes 3 and 4). Positions of molecular size standards are indicated in kilodaltons. (B) Two-hybrid analysis of full-length PKR and P58$^{IPK}$. Yeast strain Hf7c was transfected with the indicated expression constructs, and resulting clones were replica plated onto +His (top) and −His plates (bottom) as described in Materials and Methods. The −His plate contains 10 mM 3-AT. Cotransfection plasmid combination are as follows: 1, AD T antigen (Tag) (pTD1 [54])/BD-P53 (pVA3 [35]); 2, pAD-PKR K296R/pBD-P58$^{IPK}$wt; 3, pAD-PKR K296R/BD vector (pGBT9 control); 4, pAD-PKR K296R/BD-P53 (pVA3); 5, pAD-PKR K296R/BD-lamin (pLAM 5′ [6]); 6, AD vector (pGAD425 control)/pBD-P58$^{IPK}$wt; 7, AD-Tag (pTD1)/pBD-P58$^{IPK}$wt; 8, AD-lamin (pLam 5′)/pBD-P58$^{IPK}$wt. Here and in all other figures, P58$^{IPK}$ is represented by P58.

TABLE 1. Summary of β-Gal activities obtained from PKR-P58IPK and control yeast two-hybrid cotransfectants

| GAL4 construct combination | | Sp act[a] (MUG units) | Fold increase[b] |
|---|---|---|---|
| BD | AD | | |
| Vector | Vector | 5.0 | |
| P58IPKwt | Vector | 7.0 | 1.4 |
| Vector | PKR K296R | 13.5 | 2.7 |
| Vector | PKR 1-296 | 5.0 | 1.0 |
| PKR K296R | PKR 1-296 | 111.0 | 22.2 |
| P58IPKwt | PKR K296R | 114.0 | 22.8 |
| P58IPKwt | PKR 1-242 | 6.5 | 1.3 |
| P58IPKwt | PKR 244-551 | 449.0 | 89.8 |
| P58IPKwt | PKR 1-296 | 414.0 | 82.8 |
| P58IPKwt | PKR 244-366 | 488.0 | 97.6 |
| P58IPKwt | PKR 367-551 | 13.5 | 2.7 |
| P58IPKwt | PKR 244-296 | 100.0 | 20.0 |
| PKR K296R | 8-1 | 13.0 | 2.6 |
| PKR K296R | 8-2 | 117.0 | 23.4 |
| PKR K296R | ΔTPR6 | 5.0 | 1.0 |

[a] Yeast transfectants were grown in liquid medium and assayed for β-Gal activity as described previously (12, 24). Values represent the mean of two experiments for each combination.

[b] Fold increase over the values obtained from cotransfectants harboring the control AD (pGAD425) and BD (pGBT9) plasmids.

duce transcription from the *his* reporter gene. As an additional level of selectivity for two-hybrid protein interactions, we included 3-AT, a competitive inhibitor of imidazole glycerol phosphate (IGP) dehydratase (42) in the culture medium. Growth in the presence of 3-AT selects for interactions which induce His biosynthesis significantly above basal levels sufficient to overcome the 3-AT block. Such interactions will be of higher affinity and stability than interactions which do not support growth in the presence of 3-AT. We found that yeast clones coexpressing either the AD-PKR K296R or BD-P58IPKwt construct in combination with the respective control constructs failed to grow on −His medium (Fig. 2B), while clones coexpressing AD-PKR K296R and BD-P58IPKwt constructs grew on −His medium. To confirm these results, we carried out liquid β-Gal assays on the yeast cotransfectants. As summarized in Table 1, cotransfection of AD-PKR K296R and BD-P58IPKwt resulted in a strong induction of β-Gal activity, approximately equal to that of the PKR dimerization control combination of AD-PKR 1-296/BD-PKR K296R (18, 63) but significantly higher than that of the respective control cotransfections. These results collectively indicate that PKR and P58IPK interact in vivo.

PKR contains two basic regions within the amino-terminal 242 aa which participate in the binding of activating dsRNAs (26). Additionally, the PKR dsRNA-binding motifs may facilitate PKR homodimerization and interaction of PKR with other dsRNA-binding proteins by formation of a dsRNA bridge (18, 63). Using a series of AD-PKR deletion mutants (Fig. 1), coexpressed with BD-P58IPKwt, we next proceeded to map the P58IPK interactive site(s) on PKR. As shown in Fig. 3A, all AD-PKR mutant constructs were expressed in the corresponding yeast transfectants. A PKR deletion mutant, possessing the dsRNA-binding domains (without the catalytic domain), AD-PKR 1-242, failed to grow on −His medium (Fig. 3B) and failed to induce β-Gal activity above basal levels (Table 1), indicating that this construct did not interact with BD-P58IPKwt. However, mutant AD-PKR 244-551, which includes the catalytic domain but lacks the dsRNA-binding domains, interacted specifically with BD-P58IPKwt, as determined by growth on −His medium (Fig. 3B) and induction of β-Gal

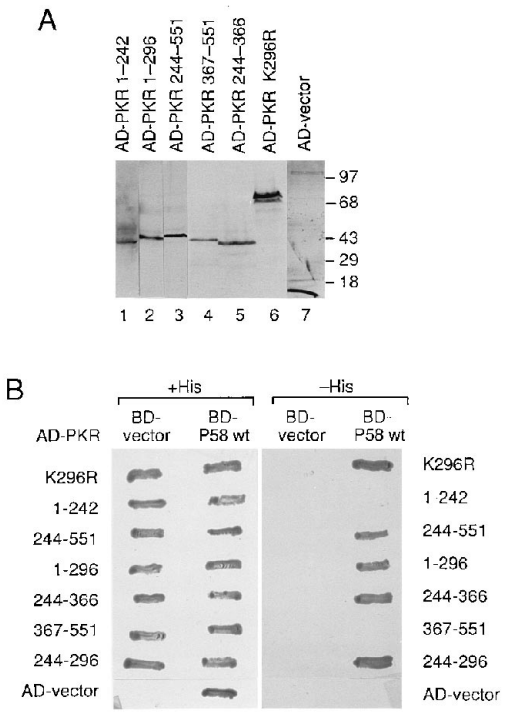


FIG. 3. Expression of PKR deletion mutants and interaction with P58IPK. (A) Expression of AD-PKR deletion constructs in yeast transfectants. Extracts from yeast transfectants harboring AD-PKR 1-242 (lane 1), AD-PKR 1-296 (lane 2), AD-PKR 244-551 (lane 3), AD-PKR 367-551 (lane 4), AD-PKR 244-366 (lane 5), AD-PKR K296R (control; lane 6), and AD vector (pGAD425 control; lane 7) were subjected to immunoblot analysis using a GAL4 AD-specific monoclonal antibody (Clontech). Not shown is AD-PKR 244-296, which we were unable to detect by this analysis. Positions of molecular size standards are indicated in kilodaltons. (B) Specific interaction of P58IPKwt with PKR deletion mutants. Yeast cells containing the empty GAL4 BD control vector pGBT9 (BD-vector) or BD-P58IPKwt (depicted in Fig. 5) were transformed with the indicated AD-PKR mutants (Fig. 1) and replica plated onto +His medium (left) and −His medium containing 8 mM 3-AT (right). As an extra control, cells expressing BD-P58IPKwt were transformed with the empty GAL4 AD control vector pGAD425 (AD-vector; bottom row). Growth on −His is indicative of interaction.

activity (Table 1). The lack of growth on −His medium exhibited by cotransfectants containing the BD vector control demonstrates the specificity of the PKR-P58IPK interaction. These results demonstrate that (i) interaction with P58IPK in vivo is independent of the PKR dsRNA-binding domains and (ii) P58IPK interacts exclusively with the carboxyl-terminal 307 aa which comprise the PKR protein kinase catalytic domain.

**P58IPK interacts with the nucleotide-binding and autoregulatory region of the PKR protein kinase catalytic domain.** To further define the P58IPK interactive region of PKR, we tested PKR deletion mutants containing discrete regions of the protein kinase catalytic domain for interaction with P58IPK in vivo. The yeast two-hybrid assay revealed that deletion mutants AD-PKR 1-296 and AD-PKR 244-366 specifically interacted with BD-P58IPKwt, as determined by growth in −His medium (Fig. 3B) and specific induction of β-Gal activity (Table 1). Transfectants co-expressing AD-PKR 367-551 and BD-P58IPKwt failed to grow on −His medium and did not induce β-Gal activity above basal levels (Fig. 3B and Table 1), indicating that P58IPK binding is independent of the PKR carboxyl-terminal 184 aa. Construct AD-PKR 367-551 did, however, mediate interaction with vaccinia virus K3L (see below), demonstrating that this PKR construct was effectively synthesized and trans-

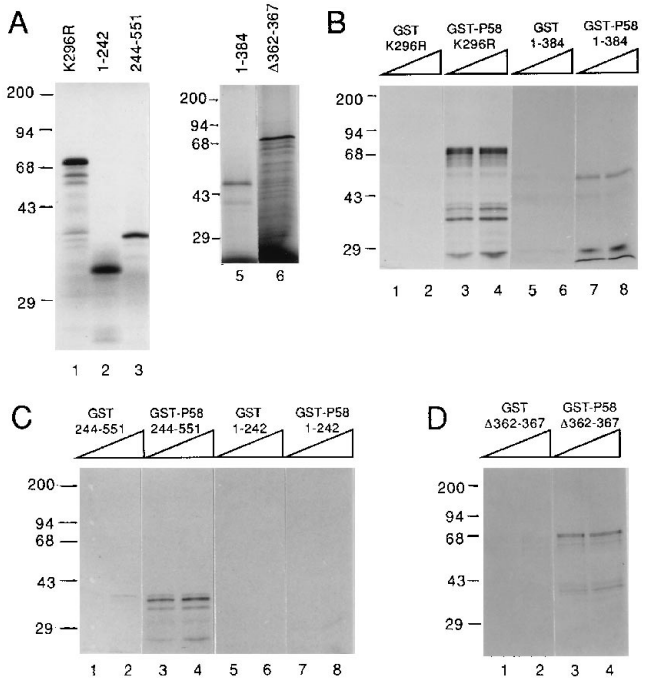


FIG. 4. In vitro binding analysis of the PKR-P58$^{IPK}$ interaction. (A) Autoradiogram from SDS-PAGE analysis of PKR in vitro translation products. Approximately $10^5$ cpm of [$^{35}$S]methionine-labeled in vitro translation product from PKR 1-551 (K296R; lane 1), 1-242 (lane 2), 244-551 (lane 3), 1-384 (lane 5), and Δ362-367 (lane 6) were run on a 12.5% acrylamide gel and subjected to autoradiography. Position of molecular size standards are indicated in kilodaltons. (B to D) Binding analysis of PKR translation products. Each panel shows an autoradiogram from SDS-PAGE analysis of PKR in vitro translation products selected by binding to GST or GST-P58$^{IPK}$. As indicated above each set of lanes, increasing amounts of *E. coli* extract containing either GST or GST-P58$^{IPK}$ (20 or 50 μl) were incubated with equal counts of [$^{35}$S]methionine-labeled in vitro PKR translation products. (B) PKR K296R (lanes 1 to 4) and PKR 1-384 (lanes 5 to 8); (C) PKR 244-551 (lanes 1 to 4) and PKR 1-242 (lanes 5 to 8); (D) PKR Δ362-367. Positions of molecular size standards are shown in kilodaltons at left of each panel.

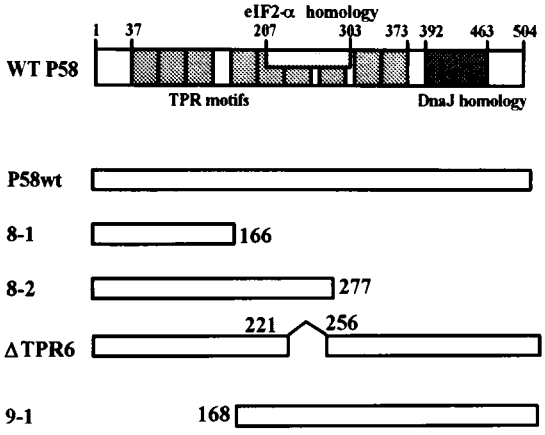


FIG. 5. Structural representation of P58$^{IPK}$ and P58$^{IPK}$ two-hybrid expression constructs. The nine tandemly arranged TPR domains are shown as 34-aa blocks. The regions of eIF2-α and DNA-J homology are shown by differential shading. The positions of terminal amino acids are indicated.

ported to the nucleus in transfected cells. It is noteworthy that AD-PKR 1-242 did not interact with BD-P58$^{IPK}$wt, while AD-PKR 1-296, which possesses an additional 54 aa (Fig. 1), did interact. Thus, to this point, all BD-P58$^{IPK}$wt-interacting constructs of AD-PKR shared 52 aa in this region (aa 244 to 296). This region of PKR includes the nucleotide-binding domain essential for protein kinase activity (protein kinase catalytic domain conservation regions I and II [reviewed in reference 28]), including the glycine-rich domain and the invariant lysine residue which cooperatively participate in binding ATP (9, 10, 74). In addition, this region contains a potential site of autophosphorylation, threonine 258, critical for kinase activation (57). To determine if PKR aa 244 to 296 defined the P58$^{IPK}$-binding motif, we tested construct AD-PKR 244-296 for in vivo interaction with BD-P58$^{IPK}$wt. As demonstrated by growth on −His medium (Fig. 3B) and induction of β-Gal activity (Table 1), construct PKR 244-296 was alone capable of a specific interaction with P58$^{IPK}$, directly demonstrating that P58$^{IPK}$ physically associates with structures spanning the nucleotide-binding and autoregulatory region of PKR.

To confirm and extend the results of the in vivo binding assays, we carried out an in vitro analysis of PKR-P58$^{IPK}$ interactions by using a GST pull-down assay. In this assay, the binding of a labeled, in vitro-translated protein to a GST fusion protein, present within a crude *E. coli* extract, is analyzed. Various PKR deletion mutants (Fig. 1) were translated in vitro in the presence of [$^{35}$S]methionine and reacted with crude extracts from *E. coli* expressing GST (as control) or GST-P58$^{IPK}$. After confirmation of the full-length synthesis of each PKR translation product by SDS-PAGE analysis (Fig. 4A), the GST pull-down assay was carried out with approximately equimolar levels of input material (Fig. 4B to D). Analysis of the bound proteins, which remained after glutathione-agarose selection and washing steps, revealed that the full-length control, PKR K296R, formed a stable complex with GST-P58$^{IPK}$ but not GST alone (Fig. 4B, lanes 1 to 4). PKR 1-384, which lacks the C-terminal 167 aa (Fig. 4B, lanes 5 to 8), and PKR 244-551, which lacks the dsRNA-binding motifs (Fig. 4C, lanes 1 to 4), bound specifically to GST-P58$^{IPK}$. Conversely, PKR 1-242 failed to mediate complex formation with GST-P58$^{IPK}$, as previously shown (66) (Fig. 4C, lanes 5 to 8). The structurally related eIF2-α kinases PKR, TIK (33), GCN2 (67), and HCR (15) all possess a conserved 6-aa motif, between conservation regions 5 and 6 (17, 28) of their respective protein kinase catalytic domains, corresponding to PKR aa 362 to 367 (LFIQME [Fig. 1]). The conservation of this motif among the eIF2-α kinases has led to speculation that this motif may play a role in substrate interaction, perhaps by mediating interaction with eIF2-α (17). To determine whether this motif is important in mediating interaction with P58$^{IPK}$, we extended our in vitro binding analyses to include an assessment of P58$^{IPK}$ binding using the PKR mutant which lacks the LFIQME motif. As shown in Fig. 4D, deletion of this region of PKR had no effect on P58$^{IPK}$ binding, as in vitro-translated mutant PKR specifically bound to GST-P58$^{IPK}$ but not GST alone. These results collectively indicate that the PKR-P58$^{IPK}$ interaction is mediated by sequences independent of the amino-terminal regulatory domains and the LFIQME sequences. Instead complex formation in vitro is dependent on structures within the first six PKR protein kinase catalytic domain conservation regions.

**Interaction with PKR in vivo requires TPR domain 6 within the eIF2-α homology region of P58$^{IPK}$.** Using our in vivo binding assay, we next set out to map the PKR-interacting domain(s) of P58$^{IPK}$. P58$^{IPK}$ is composed of several structural motifs (Fig. 5), including nine TPR motifs as well as a C-terminal DNA-J motif, both known to mediate protein-protein interactions (47, 71). In addition, the region spanning P58$^{IPK}$

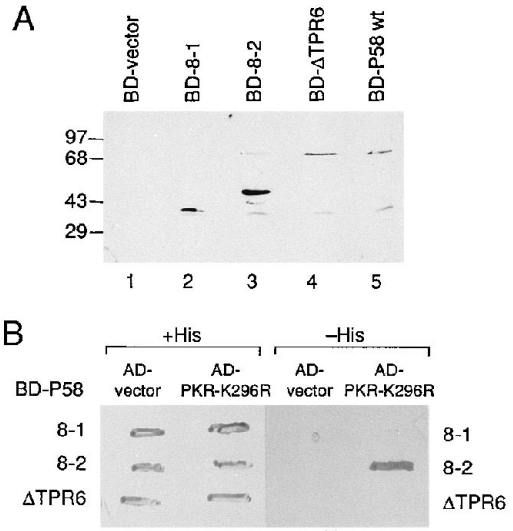


FIG. 6. Interaction with PKR requires P58IPK TPR motif 6. (A) Immunoblot analysis of BD-P58IPK yeast two-hybrid constructs. Extracts from the indicated yeast transfectants were separated by SDS-PAGE, transferred to membranes, and probed with the P58IPK-specific monoclonal antibody 2F8 (2). Lane 1, BD vector (pGBT9 control); lane 2, BD-8-1; lane 3, BD-8-2; lane 4, BD-ΔTPR6; lane 5, BD-P58IPKwt (control). Positions of molecular size standards are shown in kilodaltons. (B) Specific interaction of full-length PKR K296R with P58IPK deletion mutants. Yeast cells were cotransfected with the indicated BD-P58IPK constructs (indicated at the left and right) and the empty pGAD425 control plasmid (AD vector) or the full-length PKR mutant, AD-PKR K296R. Transfectants were replica plated onto +His medium (left) and −His medium with 5 mM 3-AT (right) and assayed for growth.

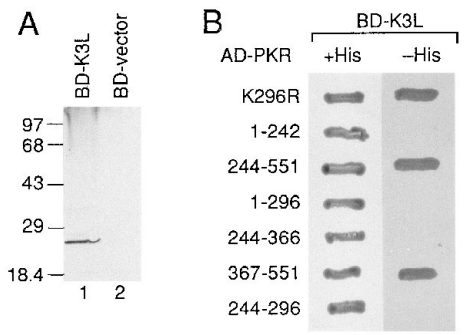


FIG. 7. Vaccinia virus K3L interacts with the PKR protein kinase catalytic domain. (A) Expression of BD-K3L in yeast transfectants. Extracts from BD-K3L (lane 1) or BD vector (control; lane 2) yeast transfectants were subjected to immunoblot analysis using a polyclonal antiserum raised against GST-K3L (gift from J. Tartaglia). Positions of molecular size standards are shown in kilodaltons at the left. (B) Specific interaction of K3L and PKR. Yeast cells expressing BD-K3L were cotransfected with the AD-PKR constructs indicated at the left. Cotransfectants were replica plated on +His medium (left) and −His medium with 12 mM 3-AT (right). Growth on −His medium is indicative of interaction.

TPR motifs 5 to 7 possesses limited homology to the natural PKR substrate, eIF2-α, including the PKR–eIF2-α consensus phosphorylation tripeptide, ELS. This region corresponds to aa 49 to 51 and 239 to 241 of eIF2-α and P58IPK, respectively (17, 51). This eIF2-α homology region (aa 207 to 303) is essential for P58IPK-mediated PKR inhibition in vitro (51, 66) as well as in vivo (73). Thus, we hypothesized that the P58IPK-PKR interaction is mediated through structures located within the P58IPK eIF2-α homology region. To test this, we prepared a series of BD-P58IPK deletion mutants (Fig. 5) which were transfected in yeast strains expressing either the negative AD control vector, pGAD425, or the full-length PKR K296R mutant fused to the GAL4 AD. P58IPK mutant constructs were expressed to approximately equal levels in yeast transfectants (Fig. 6A). Two-hybrid analysis revealed that transfectants coexpressing AD-PKR K296R and BD-8-2 (lacking the P58IPK carboxyl-terminal 227 aa) exhibited His prototrophy (Fig. 6B) and β-Gal induction (Table 1), indicating that the P58IPK carboxyl-terminal 227 aa, including the DNA-J motif, were not essential for interaction with PKR in vivo. To determine if structures within the amino-terminal 166 aa were sufficient to mediate the P58IPK-PKR association, we also tested P58IPK mutant BD-8-1 for interaction with AD-PKR K296R. Coexpression of BD-8-1 and AD-PKR K296R in the two-hybrid assay failed to induce either growth on −His medium or β-Gal expression, indicating that the P58IPK amino terminus was not sufficient to mediate interaction with PKR (Fig. 6B and Table 1).

Since we recently found that the middle portion of P58IPK, which includes the eIF2-α homology region (spanning TPR motifs 5, 6, and 7), was important for P58IPK function in vivo (73), we next tested whether this same region mediated P58IPK-PKR interactions. It is noteworthy that TPR domain 6 (aa 220 to 254) includes S241 of the ELS consensus tripeptide and that deletion of this region alone abrogates P58IPK function (73). It is therefore conceivable that P58IPK could function as a PKR substrate analog, serving as a homing signal to mediate interaction with PKR. We tested whether this region of P58IPK was required for in vivo interaction with PKR by coexpressing AD-PKR K296R with BD-P58IPK/ΔTPR6. Immunoblot analysis confirmed that construct BD-P58IPK/ΔTPR6 was efficiently expressed in yeast (Fig. 6A). Importantly, BD-P58IPK/ΔTPR6 failed to interact with PKR (Fig. 6B), as determined by failure of the corresponding clones to grow on −His medium or induce β-Gal expression (Table 1). Taken together, these results indicate that PKR interacts with the eIF2-α homology region of P58IPK and that sequences within P58IPK TPR domain six, possibly including the ELS tripeptide, are required for this interaction to occur.

**Vaccinia virus K3L forms a complex with the PKR protein kinase catalytic domain in vivo.** To gain additional insights into mechanisms of PKR down regulation, we turned our attention to the vaccinia virus-encoded PKR inhibitor, K3L. Vaccinia virus encodes a mechanism to repress the deleterious effects associated with activation of PKR in virally infected cells (7, 8, 38). Others have convincingly shown that the 88-aa product of the vaccinia virus *K3L* gene, K3L, forms a physical complex with the kinase in vitro and in vivo, leading to dramatic reductions in PKR activity (13, 18). Exhibiting a 28% amino acid identity with the amino terminus of eIF2-α (8), K3L has been proposed to inhibit PKR by functioning as an eIF2-α pseudo-substrate (8, 13). To examine the K3L interactive sites on PKR, full-length K3L was expressed in transfected yeast cells as a BD-K3L fusion protein (for immunoblot analysis, see Fig. 7A), along with several PKR mutants (Fig. 7B). Coexpression of BD-K3L with AD-PKR K296R or AD-PKR 244-551 resulted in growth on −His medium and a strong induction of β-Gal activity (Table 2), confirming that K3L and PKR interact in vivo (13, 18). These data demonstrate that the PKR protein kinase catalytic domain was sufficient to mediate this interaction. The K3L interactive domain was mapped to within aa 367 to 551 of the PKR catalytic domain, as determined by selection on −His medium and induction of β-Gal of BD-K3L transfectants coexpressing AD-PKR 367-551 (Fig. 7B and Table 2). BD-K3L transfectants coexpressing the remaining PKR catalytic domain constructs AD-PKR 244-366 and

TABLE 2. Summary of β-Gal activities obtained from PKR-K3L, P58$^{IPK}$-P58$^{IPK}$, and control yeast two-hybrid cotransfectants[a]

| GAL4 construct combination | | Sp act (MUG units) | Fold increase |
|---|---|---|---|
| BD | AD | | |
| K3L | Vector | 13.0 | 2.6 |
| K3L | PKR K296R | 635.0 | 127.0 |
| K3L | PKR 1-242 | 8.5 | 1.7 |
| K3L | PKR 1-296 | 4.5 | 1.0 |
| K3L | PKR 244-296 | 9.0 | 1.8 |
| K3L | PKR 244-551 | 364.0 | 72.8 |
| K3L | PKR 244-366 | 11.0 | 2.2 |
| K3L | PKR 367-551 | 912.5 | 182.5 |
| P58$^{IPK}$wt | 8-1 | 327.5 | 65.5 |
| P58$^{IPK}$wt | 8-2 | 366.0 | 73.2 |
| P58$^{IPK}$wt | 9-1 | 10.0 | 2.0 |

[a] Each value is the mean of two experiments. See Table 1 footnotes for experimental details.

AD-PKR 244-296 failed to grow on −His medium or induce β-Gal above basal levels. Similarly, and consistent with a previous report (18), the amino-terminal PKR constructs, AD-PKR 1-242 and AD-PKR 1-296, did not mediate interaction with BD-K3L, as transfectants coexpressing these constructs failed to grow on −His medium and lacked β-Gal activity. Our previous analysis indicated that P58$^{IPK}$ interacted with constructs AD-PKR 1-296, AD-PKR 244-366, and AD-PKR 244-296 (Fig. 3), demonstrating that these proteins were efficiently expressed and localized to the nucleus of transfected cells. Thus, the failure of BD-K3L to interact with these AD-PKR constructs cannot be attributed to poor expression or failure to localize to the yeast cell nucleus. Collectively, these results demonstrate that like P58$^{IPK}$, K3L interacts exclusively with the PKR protein kinase catalytic domain. However, unlike P58$^{IPK}$, which associates with structures within protein kinase catalytic domain homology region II (PKR aa 244 to 296), the K3L interactive region of PKR broadly maps to a nonoverlapping domain within the carboxyl-terminal 184 aa, corresponding to protein kinase catalytic domain homology regions VI to XI (28), which are predicted to participate in substrate recognition and binding (10, 28, 74).

**P58$^{IPK}$ can self-associate in vivo.** Structural three-dimensional modeling predicts that the individual TPR motifs in TPR-containing proteins functionally cooperate to mediate intra- and intermolecular interactions by assuming a TPR-specific "knob-in-hole" structure (25, 31, 47). Thus, one would predict that multimerization is a characteristic of this protein family. Indeed, the structurally related TPR proteins Cdc16, Cdc23, and Cdc27 of *S. cerevisiae* participate in TPR-dependent interactions in vivo, including homodimerization and formation of an essential mitotic heterotrimeric complex (46). To determine if P58$^{IPK}$ formed homotypic complexes in vivo, we coexpressed various AD-P58$^{IPK}$ deletion constructs with BD-P58$^{IPK}$wt in yeast cells and subjected the transfectants to the two-hybrid assay. Immunoblot analysis confirmed that constructs AD-8-2, AD-8-1, and AD-9-1 were expressed at approximately equal efficiencies (Fig. 8A). Coexpression of AD-8-2 and BD-P58$^{IPK}$wt resulted in growth on −His medium (Fig. 8B) and a strong induction of β-Gal activity (Table 2), indicating that (i) P58$^{IPK}$, like other TPR proteins, is capable of homotypic interaction in vivo and (ii) P58$^{IPK}$ homotypic interaction does not depend upon the P58$^{IPK}$ carboxyl-terminal 227 aa, including structures located in the P58$^{IPK}$ DNA-J motif. To further define the region of homotypic interaction, we tested

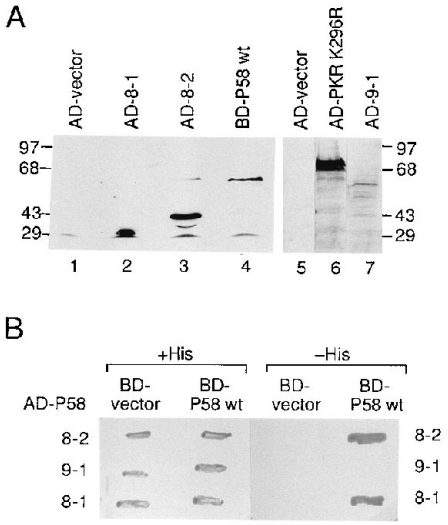


FIG. 8. P58$^{IPK}$ self-associates in vivo. (A) Expression of AD-P58$^{IPK}$ mutant constructs in yeast transfectants. Extracts from the indicated yeast transfectants were subjected to immunoblot analysis using either the P58$^{IPK}$-specific monoclonal antibody 2F8 (lanes 1 to 4) or the GAL4 AD-specific monoclonal antibody (lanes 5 to 7). Lanes 1 and 5, AD vector (pGAD425 control); lane 2, AD-8-1; lane 3, AD-8-2; lane 4, BD-P58$^{IPK}$wt (control); lane 6, AD-PKR K296R (control); lane 7, AD-9-1. Positions of molecular size standards are indicated in kilodaltons. (B) Self-association of P58$^{IPK}$. Cells were cotransfected with the indicated AD-P58$^{IPK}$ constructs (indicated at the left and right) and the BD control plasmid pGBT9 (BD-vector) or BD-P58$^{IPK}$wt and replica plated onto +His medium (left) and −His medium with 10 mM 3-AT (right). Interaction was determined by growth on −His medium.

P58$^{IPK}$ deletion construct AD-8-1, possessing only the P58$^{IPK}$ amino-terminal 166 aa (Fig. 5), for the ability to interact with BD-P58$^{IPK}$wt in vivo. Coexpression of AD-8-1 with BD-P58$^{IPK}$wt resulted in growth on −His medium (Fig. 8B), which was confirmed by analysis of β-Gal activity (Table 2). We next tested the reciprocal construct, AD-9-1, which lacks the amino-terminal 167 aa of P58$^{IPK}$, for the ability to interact with BD-P58$^{IPK}$wt. As shown in Fig. 8B and Table 2, deletion of the amino-terminal 167 aa of P58$^{IPK}$ prevented homotypic interaction in vivo, as clones coexpressing AD-9-1 and BD-P58$^{IPK}$wt failed to induce reporter gene expression, determined by lack of growth on −His medium and low β-Gal activity. BD vector control cotransfectants did not grow on −His medium (Fig. 8B). Taken together, these data demonstrate that P58$^{IPK}$ can form specific homotypic complexes in vivo in which the amino-terminal 166 aa are both necessary and sufficient for mediating this homotypic interaction. Inclusion of P58$^{IPK}$ TPR domains 1 to 3, as well a portion of TPR domain 4 (Fig. 5), within the amino-terminal 166 aa suggests that formation of a P58$^{IPK}$ complex may be a TPR domain-mediated event.

## DISCUSSION

PKR and P58$^{IPK}$ each play an important role in the regulation of viral gene expression in virus-infected cells. PKR is a component of the host interferon defense mechanisms designed to restrict virus replication (37, 38). However, to counteract these effects, viruses have evolved strategies to down regulate PKR. Influenza virus accomplishes this by activating the cellular PKR inhibitor, P58$^{IPK}$ (40, 51, 52). Several studies also have ascribed a tumor suppressor role to PKR, as coexpression of dominant negative PKR mutants leads to malignant transformation of mammalian cells (5, 43, 62). In accor-

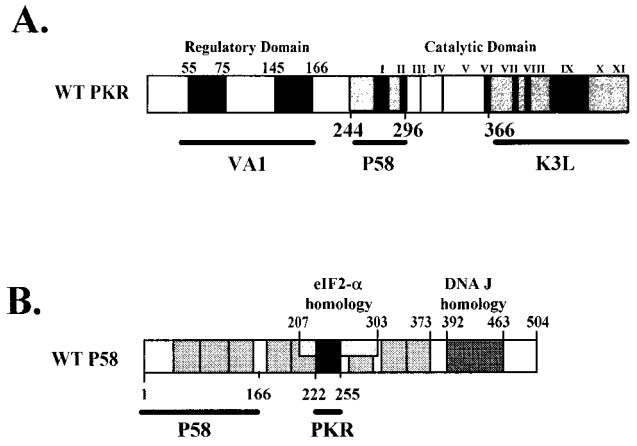


FIG. 9. Locations of the interactive domains of PKR and P58IPK. (A) Wild-type (wt) PKR. PKR interaction with the adenovirus VAI RNA has been mapped to dsRNA-binding domain-inclusive N-terminal regulatory region (39, 41, 58). The P58IPK and K3L interactive domains both localize to nonoverlapping regions within the PKR protein kinase catalytic domain (shaded). The P58IPK-interacting domain spans aa 244 to 296, which include protein kinase catalytic domain homology regions I and II (28) as well as a preceding region important for PKR activation (57). The K3L-interacting domain lies within aa 367 to 551, including kinase homology domains VI to XI. Bars indicate positions of the interactive domains. (B) P58IPK. Complex formation and interaction with PKR are mediated by distinct nonoverlapping domains within P58IPK. Homotypic complex formation is mediated by structures within the amino-terminal 166 aa which include TPR domains 1 to 3 as well as a portion of TPR domain 4. Interaction with PKR maps to the 34 aa within TPR motif 6 (shown in black), which includes the eIF2-α consensus ELS tripeptide corresponding serine 51 of eIF2-α (51). Bars indicate the region spanning the interactive domains.

dance with these data, P58IPK possess oncogenic potential, in that overexpression in NIH 3T3 cells leads to malignant transformation, possibly via a P58IPK-mediated inhibition of the PKR tumor suppressor phenotype (2). Thus, mechanisms which regulate activity of PKR can have dramatic effects on the cell by influencing the growth-suppressive and antiviral activity of the enzyme. Finally, PKR has been implicated in the control of other pathways, including transcriptional activation (45) and induction of apoptosis (50). The diverse roles played by PKR prompted the current study, which was designed to determine the molecular mechanisms of kinase inhibition.

We found that P58IPK and K3L interacted with the PKR protein kinase catalytic domain, indicating that the PKR dsRNA-binding domains were dispensable for these interactions. This finding is in accordance with our previous results showing that a full-length mutant PKR, deficient in dsRNA binding, could still interact with P58IPK (66). This finding contrasts dramatically with observations regarding adenovirus-encoded VAI RNA, which interacts with the PKR amino-terminal regulatory domains (39, 41, 58) and functions to inhibit PKR through competitive inhibition of dsRNA binding. Our results localize the minimal P58IPK interactive site(s) on PKR to the 52-aa region comprising aa 244 to 296 (Fig. 9A). This P58IPK interactive domain of PKR covers protein kinase catalytic domain homology regions I and II (reviewed by Hanks et al. [28]), which contain the glycine-rich motif GxGxxG and the invariant lysine residue (K-296) which participate in nucleotide binding. It is tempting to speculate that by binding to this region of the kinase, P58IPK could mediate its inhibitory effects by interfering with the nucleotide binding reaction either directly or indirectly by inducing PKR steric alterations. Additionally, the former effect could also interfere with critical regulatory phosphorylation events, which include autophosphorylation of T-258 within the P58IPK interactive region of PKR (57). While it is not known at this time if P58IPK binds to monomeric and/or multimeric forms of PKR, binding of P58IPK to PKR could prevent formation of an active PKR complex or, alternatively, disrupt preformed active PKR homotypic complexes, thus inhibiting the crucial PKR autoactivation step which may be a prerequisite for PKR function.

In contrast to P58IPK, the interaction between PKR and K3L was localized to PKR aa 367 to 551 (Fig. 9A), indicating that these inhibitors employ divergent mechanisms of PKR inhibition. This region of PKR does not include the complete LFIQME motif conserved among the eIF2-α kinase family (17), which has been postulated to mediate the K3L-PKR interaction. This finding suggests that this motif is not essential for K3L binding and thus may not be part of a consensus substrate recognition site. Similarly, the LFIQME motif was not essential for P58IPK-PKR interactions. On the basis of the crystal structures of various eukaryotic protein kinases, PKR aa 367 to 551 localize to within the large lobe of the generalized three-dimensional structure predicted for the PKR protein kinase catalytic domain, while aa 244 to 296 occupy a distinct region of the small lobe involved in nucleotide binding (10, 74) and autophosphorylation. The large lobe of the eukaryotic protein kinase catalytic domain is largely responsible for substrate recognition and binding, although certain conserved residues contribute to nucleotide binding as well (74). Thus, K3L, which shares homology with the amino terminus of eIF2-α (8), may inhibit PKR function by blocking the PKR-substrate interaction. Functioning as a high-affinity PKR pseudo-substrate, K3L could essentially irreversibly bind to the substrate recognition site of PKR to render the kinase inactive. Identification of the precise PKR substrate-binding site will allow for further definition of the mechanisms by which K3L mediates inhibition of PKR.

The PKR-interactive region of P58IPK was independent of both the amino- and carboxyl-terminal regions of the inhibitor and was mapped to the P58IPK eIF2-α homology domain (Fig. 9B). Homology with eIF2-α, within the PKR interactive region, is limited to approximately 31% amino acid identity (including gaps) over a 97-aa region (51). This region includes the PKR consensus eIF2-α phosphorylation motif, ELS (P58IPK aa 239 to 241), which localizes to P58IPK TPR domain 6. Importantly, we also recently found that TPR domain 6 is critical for P58IPK function inside the cell (73). P58IPK TPR domain 6 contains the ELS tripeptide, suggesting that P58IPK may function as a pseudo-substrate, binding to the PKR substrate-binding domain and blocking interaction with the natural PKR substrate eIF2-α, an event which would require the presence of S-241 to functionally mimic eIF2-α. However, in direct conflict with this notion, we previously found that a P58IPK S241A mutant was still able to inhibit PKR activity (51), indicating that S-241 was not essential for function. Taken together, these results suggest that, rather than functioning as a PKR pseudo-substrate, the sequences within P58IPK TPR domain 6 comprise a PKR homing signal which serves to direct P58IPK to the kinase. It is worth noting other TPR proteins which form heterotypic protein-protein interactions mediated specifically by the TPR domains. For example, the Cyc8-Tup1 interaction in yeast strains is TPR specific, mediated by the Cyc8 TPR domains (76). Interestingly, this interaction required a specific combination of Cyc8 TPR motifs, indicating that these domains are not functionally redundant. Similarly, the interaction between the human nuc2 and retinoblastoma protein required a crucial nuc2 TPR domain (16).

In addition to interacting with PKR, P58IPK can self-associate, forming a homotypic complex in the two-hybrid assay. However, we cannot formally exclude the possibility that the

$P58^{IPK}$ homotypic interaction seen in the two-hybrid assay is actually mimicking an intramolecular association rather than a true intermolecular event. In either case, while interactions with PKR were exclusive of the amino-terminal region of $P58^{IPK}$ (spanning complete TPR motifs 1 to 4 and a portion of TPR motif 5), we found that this region was both necessary and sufficient to mediate $P58^{IPK}$ self-association in our two-hybrid assay (Fig. 9B). Other TPR proteins have the ability to mediate homotypic interactions in vivo. Perhaps the best-characterized interactions between TPR proteins are those between Cdc16, Cdc23, and Cdc27, which form a complex essential for mitosis (46). In this case, complete complex formation could be mapped to an essential TPR domain in Cdc27. Mutations in this region of Cdc27 did not affect self-association or the ability to associate with Cdc16 but instead reduced interactions with Cdc23. These studies collectively indicate that TPR proteins can participate in both homotypic and heterotypic protein-protein interactions, including those directly mediated by TPR domains. Self-association of $P58^{IPK}$ is mediated by aa 1 to 166, composed of TPR domains 1 to 3 (and a portion of TPR domain 4), suggesting that $P58^{IPK}$ self-association is similarly a TPR-mediated event. Currently, we do not know the significance of the $P58^{IPK}$ self-association or whether $P58^{IPK}$ intra- or intermolecular complex formation is required for PKR binding and/or kinase inhibitory activity. Conceivably, $P58^{IPK}$ self-association could impart other, yet undefined functions to $P58^{IPK}$.

$P58^{IPK}$ itself is regulated by complex formation with its own inhibitor, I-$P58^{IPK}$ (52). It is only after specific events, such as infection by influenza virus (40) or biochemical fractionation (53), that the latent PKR inhibitory activity of $P58^{IPK}$ is unmasked as a result of dissociation from its inhibitory complex. While the molecular mechanisms of $P58^{IPK}$ regulation are still unknown, we have recently isolated a novel cDNA encoding a $P58^{IPK}$-interacting protein which has limited homology to mammalian isoforms of heat shock protein 90 and possesses $P58^{IPK}$-regulatory properties (23). Studies are in progress to define the role of this novel $P58^{IPK}$ interaction. Currently, we propose a model for the regulation of PKR by $P58^{IPK}$ whereby the PKR-inhibitory activity of $P58^{IPK}$ is activated by dissociation from an inhibitory complex. Active $P58^{IPK}$, whether singularly or as a $P58^{IPK}$ homotypic complex, binds to PKR within the nucleotide-binding and regulatory region, defined by PKR aa 244 to 296, with a resultant inhibition of PKR activity. It is tempting to speculate that $P58^{IPK}$ is a component of the stress/heat shock response pathway and that influenza virus has evolved mechanisms to intersect with this pathway to ensure its efficient gene expression and replication.

## ACKNOWLEDGMENTS

We thank Dagmar Daniel for help in preparing the manuscript, and Marjorie Domenowske for figure preparation. We thank Glen Barber and Rosemary Jagus for providing PKR mutants and BD-K3L, respectively. We are grateful to Norina Tang for providing the $P58^{IPK}$ ΔTPR6 mutant construct. James Tartaglia provided the K3L antisera.

This work was supported by National Institutes of Health grants AI 22646 and RR 00166 to M.G.K. M.G. was supported by National Institutes of Health training grant CA 09229-18 and is currently a Helen Hay Whitney Fellow.

## REFERENCES

1. **Aprelikova, O., Y. Xiong, and E. T. Liu.** 1995. Both p16 and p21 families of cyclin-dependent kinase (CDK) inhibitors block the phosphorylation of cyclin-dependent kinases by the CDK-activating kinase. J. Biol. Chem. **270:** 18195–18197.
2. **Barber, G. N., S. Thompson, T.-G. Lee, T. Strom, A. Daveau, and M. G. Katze.** 1994. The 58KDa inhibitor of the interferon-induced dsRNA activated protein kinase (PKR) is a TPR protein with oncogenic properties. Proc. Natl. Acad. Sci. USA **91:**4278–4282.
3. **Barber, G. N., J. Tomita, M. S. Garfinkel, A. G. Hovanessian, E. Meurs, and M. G. Katze.** 1992. Detection of protein kinase homologues and viral RNA binding domains utilizing polyclonal antiserum prepared against a baculovirus expressed dsRNA activated 68,000 dalton protein kinase. Virology **191:** 670–679.
4. **Barber, G. N., J. Tomita, A. G. Hovanessian, E. Meurs, and M. G. Katze.** 1991. Functional expression and characterization of the interferon-induced double-stranded RNA activated P68 protein kinase from *Escherichia coli*. Biochemistry **30:**10356–10361.
5. **Barber, G. N., M. Wambach, S. Thompson, R. Jagus, and M. G. Katze.** 1995. PKR protein kinase mutants lacking double-stranded RNA binding domain I can act as transdominant inhibitors and induce malignant transformation. Mol. Cell. Biol. **15:**3138–3146.
6. **Bartel, P. L., C.-T. Chien, R. Sternglanz, and S. Fields.** 1993. Using the two-hybrid system to detect protein-protein interactions, p. 153–179. *In* D. A. Hartley (ed.), Cellular interactions in development: a practical approach. Oxford University Press, Oxford.
7. **Beattie, E., E. Paoletti, and J. Tartaglia.** 1995. Distinct patterns of IFN sensitivity observed in cells infected with vaccinia K3L- and E3L-mutant viruses. Virology **210:**254–263.
8. **Beattie, E., J. Tartaglia, and E. Paoletti.** 1991. Vaccinia virus-encoded eIF-2 alpha homolog abrogates the antiviral effect of interferon. Virology **183:**419–422.
9. **Bossemeyer, D.** 1994. The glycine-rich sequence of protein kinases: a multifunctional element. Trends Biochem. Sci. **19:**201–205.
10. **Bossemeyer, D.** 1995. Protein kinases—structure and function. FEBS. Lett. **369:**57–61.
11. **Cabanillas, F., S. Pathak, J. Trujillo, J. Manning, R. Katz, P. McLaughlin, W. S. Velasquez, F. B. Hagemeister, A. Goodacre, A. Cork, J. J. Butler, and E. J. Freireich.** 1988. Frequent non-random chromosome abnormalities in 27 patients with untreated large cell lymphoma and immunoblastic lymphoma. Cancer Res. **48:**5557–5564.
12. **Cao, J., and A. P. Geballe.** 1994. Mutational analysis of the translational signal in the human cytomegalovirus gpUL4 (gp48) transcript leader by retroviral infection. Virology **205:**151–160.
13. **Carroll, K., O. Elroy-Stein, R. Moss, and R. Jagus.** 1993. Recombinant vaccinia virus K3L gene product prevents activation of dsRNA dependent eIF 2 kinase. J. Biol. Chem. **268:**12837–12842.
14. **Chang, H.-W., J. C. Watson, and B. L. Jacobs.** 1992. The E3L gene of vaccinia virus encodes and inhibition of the interferon induced, dsRNA dependent protein kinase. Proc. Natl. Acad. Sci. USA **89:**4825–4829.
15. **Chen, J., J. Pal, M. S. Throop, L. Gehrke, I. Kuo, J. K. Pal, M. Brodsky, and I. M. London.** 1991. Cloning of the cDNA of the heme-regulated eukaryotic initiation factor 2α (eIF-2α) kinase of rabbit reticulocytes: homology to yeast GCN2 protein kinase and human double-stranded-RNA-dependent eIF2-α kinase. Proc. Natl. Acad. Sci. USA **88:**7729–7733.
16. **Chen, P. L., Y. Ueng, T. Durfee, K.-C. Chen, T. Yang-Feng, and W.-H. Lee.** 1995. Identification of a human homologue of yeast nuc2 which interacts with the retinoblastoma protein in a specific manner. Cell Growth Differ. **6:**199–210.
17. **Chong, K. L., K. Schappert, E. Meurs, F. Feng, T. F. Donahue, J. D. Friesen, A. G. Hovanessian, and B. R. G. Williams.** 1992. Human P68 kinase exhibits growth suppression in yeast and homology to the translational regulator GCN2. EMBO J. **11:**1553–1562.
18. **Cosentino, G. P., S. Venkatesan, F. C. Serluca, S. R. Green, M. B. Mathews, and N. Sonenberg.** 1995. Double-stranded-RNA-dependent protein kinase and TAR RNA-binding protein form homo- and heterodimers in vivo. Proc. Natl. Acad. Sci. USA **92:**9445–9449.
19. **Draetta, G.** 1990. Cell cycle control in eukaryotes: molecular mechanisms of cdc2 activation. Trends Biochem. Sci. **15:**378–383.
20. **Estojak, J., R. Brent, and E. A. Golemis.** 1995. Correlation of two-hybrid affinity data with in vitro measurements. Mol. Cell. Biol. **15:**5820–5829.
21. **Fields, S., and O. Song.** 1989. A novel genetic system to detect protein-protein interactions. Nature (London) **340:**245–246.
22. **Galabru, J., and A. G. Hovanessian.** 1987. Autophosphorylation of the protein kinase dependent on double-stranded RNA. J. Biol. Chem. **262:**15538–15544.
23. **Gale, M., and M. Katze.** 1996. Unpublished data.
24. **Geballe, A. P., and E. S. Mocarski.** 1988. Translational control of cytomegalovirus gene expression is mediated by upstream AUG codons. J. Virol. **62:**3334–3340.
25. **Goebl, M., and M. Yanagida.** 1991. The TPR snap helix: a novel pretein repeat motif from mitosis to transcription. Trends Biochem. Sci. **16:**173–177.
26. **Green, S. R., and M. B. Mathews.** 1992. Two RNA binding motifs in the double-stranded RNA activated protein kinase, DAI. Genes Dev. **6:**2478–2490.
27. **Guan, K.-L., C. W. Jenkins, Y. Li, M. A. Nichols, X. Wu, C. L. O'Keefe, A. G. Matera, and Y. Xiong.** 1994. Growth suppression by p18, a $p16^{INK4/MTS1}$- and $p14^{INK4B/MTS2}$-related CDK6 inhibitor, correlates with wild-type pRb function. Genes Dev. **8:**2939–2952.

28. **Hanks, S. K., A. M. Quinn, and T. Hunter.** 1988. The protein kinase family: conserved features and deduced phylogeny of the catalytic domains. Science **241:**42–52.
29. **Harper, J. W., G. R. Adami, N. Wei, K. Keyomarsi, and S. J. Elledge.** 1993. The p21 Cdk-interacting protein Cip1 is a potent inhibitor of G1 cyclin-dependent kinases. Cell **75:**805–816.
30. **Hershey, J. W. B.** 1991. Translational control in mammalian cells. Annu. Rev. Biochem. **60:**717–755.
31. **Hirano, T., N. Kinoshita, M. Morikawa, and M. Yanagida.** 1990. Snap helix with knob and hole: essential repeats in *S. pombe* nuclear protein nuc2+. Cell **60:**319–328.
32. **Huang, S., W. Hendriks, A. Althage, S. Hemmi, H. Bluethmann, R. Kamijo, J. Vilcek, R. M. Zinkernagel, and M. Aguet.** 1993. Immune response in mice that lack the interferon-γ receptor. Science **259:**1742–1745.
33. **Icely, P. L., P. Gros, J. J. M. Bergeron, A. Devault, D. E. H. Afar, and J. C. Bell.** 1991. TIK, a novel serine/threonine kinase, is recognized by antibodies directed against phosphotyrosine. J. Biol. Chem. **266:**16073–16077.
34. **Imani, F., and B. L. Jacobs.** 1988. Inhibitory activity for the interferon-induced protein kinase is associated with the reovirus serotype 1 sigma 3 protein. Proc. Natl. Acad. Sci. USA **85:**7887–7891.
35. **Iwabachi, K., B. Li, P. Bartel, and S. Fields.** 1996. Use of the two-hybrid system to identify the domain of P53 involved in oligomerization. Oncogene **8:**1693–1696.
36. **Katze, M. G.** 1992. The war against the interferon-induced dsRNA activated protein kinase: can virus win? J. Interferon Res. **12:**241–248.
37. **Katze, M. G.** 1993. Games viruses play: a strategic initiative against the interferon-induced dsRNA activated 68,000 Mr protein kinase. Semin. Virol. **4:**259–268.
38. **Katze, M. G.** 1995. Regulation of the interferon induced-PKR: can viruses cope? Trends Microbiol. **3:**75–78.
39. **Katze, M. G., D. DeCorato, B. Safer, J. Galabru, and A. G. Hovanessian.** 1987. Adenovirus VAI RNA complexes with the 68,000 Mr protein kinase to regulate its autophosphorylation and activity. EMBO J. **6:**689–697.
40. **Katze, M. G., J. Tomita, T. Black, R. M. Krug, B. Safer, and A. G. Hovanessian.** 1988. Influenza virus regulates protein synthesis during infection by repressing the autophosphorylation and activity of the cellular 68,000-$M_r$ protein kinase. J. Virol. **62:**3710–3717.
41. **Katze, M. G., M. Wambach, M.-L. Wong, M. S. Garfinkel, E. Meurs, K. L. Chong, B. R. G. Williams, A. G. Hovanessian, and G. N. Barber.** 1991. Functional expression of interferon-induced, double-stranded RNA-activated 68,000-$M_r$ protein kinase in a cell-free system. Mol. Cell. Biol. **11:** 5497–5505.
42. **Kishore, G. M., and D. M. Shaw.** 1988. Amino acid biosynthesis inhibitors as herbicides. Annu. Rev. Biochem. **57:**627–663.
43. **Koromilas, A. E., S. Roy, G. N. Barber, M. G. Katze, and N. Sonneberg.** 1992. Malignant transformation of the IFN-inducible dsRNA dependent protein kinase. Science **257:**1685–1689.
44. **Korth, M. J., C. N. Lyons, M. Wambach, and M. G. Katze.** 1996. Cloning, expression, and cellular localization of the oncogenic 58-kDa inhibitor of the RNA-activated human and mouse protein kinase. Gene **170:**181–188.
45. **Kumar, A., J. Haque, J. Lacoste, J. Hiscott, and B. R. G. Williams.** 1994. The dsRNA-dependent protein kinase, PKR, activates transcription factor NF-kB by phosphorylating IkB. Proc. Natl. Acad. Sci. USA **91:**6288–6292.
46. **Lamb, J. R., W. A. Michaud, R. S. Sikorski, and P. A. Hieter.** 1994. Cdc16p, Cdc23p and Cdc27p form a complex essential for mitosis. EMBO J. **13:**4321–4328.
47. **Lamb, J. R., S. Tugendreich, and P. Hieter.** 1995. Tetratrico peptide repeat interactions: to TPR or not to TPR? Trends Biochem. Sci. **20:**257–259.
48. **Langland, J. O., and B. L. Jacobs.** 1992. Cytosolic double-stranded RNA-dependent protein kinase is likely a dimer of partially phosphorylated Mr=66,000 subunits. J. Biol. Chem. **267:**10729–10736.
49. **Laurent, A. G., B. Krust, J. Galabru, J. Svab, and A. G. Hovanessian.** 1985. Monoclonal antibodies to interferon induced 68,000 Mr protein and their use for the detection of double-stranded RNA dependent protein kinase in human cells. Proc. Natl. Acad. Sci. USA **82:**4341–4345.
50. **Lee, S. B., and M. Esteban.** 1994. The interferon-induced double-stranded RNA-activated protein kinase induces apoptosis. Virology **199:**491–496.
51. **Lee, T. G., N. Tang, S. Thompson, J. Miller, and M. G. Katze.** 1994. The 58,000-dalton cellular inhibitor of the interferon-induced double-stranded RNA-activated protein kinase (PKR) is a member of the TPR repeat family of proteins. Mol. Cell. Biol. **14:**2331–2342.
52. **Lee, T. G., J. Tomita, A. G. Hovanessian, and M. G. Katze.** 1990. Purification and partial characterization of a cellular inhibitor of the interferon-induced 68,000 Mr protein kinase from influenza virus-infected cells. Proc. Natl. Acad. Sci. USA **87:**6208–6212.
53. **Lee, T. G., J. Tomita, A. G. Hovanessian, and M. G. Katze.** 1992. Characterization and regulation of the 58,000-dalton cellular inhibitor of the interferon-induced, dsRNA-activated protein kinase. J. Biol. Chem. **267:**14238–14243.
54. **Li, B., and S. Fields.** 1993. Identification of mutations in P53 that affect its binding to SV40 T antigen by using the yeast two-hybrid system. FASEB J. **7:**957–963.
55. **Lu, P.-K., S. A. Osmani, and A. R. Means.** 1993. Properties and regulation of the cell cycle-specific NIMA protein kinase of *Aspergillus nidulans*. J. Biol. Chem. **268:**8769–8776.
56. **Luo, Y., J. Hurwitz, and J. Massague.** 1995. Cell-cycle inhibition by independent CDK and PCNA binding domains in p21$^{Cip1}$. Nature (London) **375:**159–162.
57. **Mathews, M. B.** 1996. Personal communication.
58. **McCormack, S. J., and C. E. Samuel.** 1995. Mechanism of interferon action: RNA-binding activity of full-length and R-domain forms of the RNA-dependent protein kinase PKR—determination of $K_D$ values for $VA_I$ and TAR RNAs. Virology **206:**511–519.
59. **McMillan, N. A. J., R. F. Chun, D. P. Siderovski, J. Galabru, W. M. Toone, C. E. Samuel, T. W. Mak, A. G. Hovanessian, K.-T. Jeang, and B. R. G. Williams.** 1995. HIV-1 Tat directly interacts with the interferon-induced, double-stranded RNA-dependent kinase, PKR. Virology **213:**413–424.
60. **Merrick, W. C.** 1992. Mechanism and regulation of eukaryotic protein synthesis. Microbiol. Rev. **56:**291–315.
61. **Meurs, E., K. L. Chong, J. Galabru, N. Thomas, I. Kerr, B. R. G. Williams, and A. G. Hovanessian.** 1990. Molecular cloning and characterization of the human double-stranded RNA-activated protein kinase induced by interferon. Cell **62:**379–390.
62. **Meurs, E. F., J. Galabru, G. N. Barber, M. G. Katze, and A. G. Hovanessian.** 1993. Tumor suppressor function of the interferon-induced double-stranded RNA-activated protein kinase. Proc. Natl. Acad. Sci. USA **90:**232–236.
63. **Patel, R. C., P. Stanton, N. M. J. McMillan, B. R. G. Williams, and G. C. Sen.** 1995. The interferon-inducible double-stranded RNA-activated protein kinase self-associates *in vitro* and *in vivo*. Proc. Natl. Acad. Sci. USA **92:**8283–8287.
64. **Pelech, S. L., and J. S. Sanghera.** 1992. Mitogen-activated protein kinases: versatile transducers for cell signaling. Trends Biochem. Sci. **17:**232–237.
65. **Polyak, K., M.-H. Lee, H. Erdjument-Bromage, A. Koff, J. M. Roberts, P. Tempst, and J. Massague.** 1994. Cloning of p27$^{Kip1}$, a cyclin-dependent kinase inhibitor and a protein mediator of extracellular antimitogenic signals. Cell **78:**59–66.
66. **Polyak, S. J., N. Tang, M. Wambach, G. N. Barber, and M. G. Katze.** 1996. The p58 cellular inhibitor complexes with the interferon-induced, double-stranded RNA-dependent protein kinase, PKR, to regulate its autophosphorylation and activity. J. Biol. Chem. **271:**1702–1707.
67. **Ramirez, M., R. C. Wek, and A. G. Hinnebusch.** 1991. Ribosome association of GCN2 protein kinase, a translational activator of the GCN4 gene of *Saccharomyces cerevisiae*. Mol. Cell Biol. **11:**3027–3036.
68. **Rhoads, R. E.** 1993. Regulation of eukaryotic protein synthesis by initiation factors. J. Biol. Chem. **268:**3017–3020.
69. **Roy, S., M. G. Katze, N. T. Parkin, I. Edery, A. G. Hovanessian, and N. Sonenberg.** 1990. Control of the interferon-induced 68-kilodalton protein kinase by the HIV-1 *tat* gene product. Science **247:**1216–1219.
70. **Samuel, C. E.** 1991. Antiviral actions of interferon interferon-regulated cellular proteins and their surprisingly selective antiviral activities. Virology **183:**1–11.
71. **Silver, P. A., and J. C. Way.** 1993. Eukaryotic DnaJ homologs and the specificity of Hsp70 activity. Cell **74:**5–6.
72. **Smith, D. B., and K. S. Johnson.** 1988. Single-step purification of polypeptides expressed in *Escherichia coli* as fusions with glutathione-*S*-transferase. Gene **67:**31–40.
73. **Tang, N., C. Y. Ho, and M. G. Katze.** The 58 kDa inhibitor of the dsRNA-dependent protein kinase (PKR) requires the TPR6 and DnaJ motifs to stimulate protein synthesis in vivo. Submitted for publication.
74. **Taylor, S. S., D. R. Knighton, J. Zheng, J. M. Sowadski, C. S. Gibbs, and M. J. Zoller.** 1993. A template for the protein kinase family. Trends Biochem. Sci. **18:**84–89.
75. **Thomis, D. C., and C. E. Samuel.** 1993. Mechanism of interferon action: evidence for intermolecular autophosphorylation and autoactivation of the interferon-induced, RNA-dependent protein kinase PKR. J. Virol. **67:**7695–7700.
76. **Tzamarias, D., and K. Struhl.** 1995. Distinct TPR motifs of Cyc8 are involved in recruiting the Cyc8-Tup1 corepressor complex to differentially regulated promoters. Genes Dev. **9:**821–831.